

# Microfluidic Formation of Monodispersed Spherical Microgels Composed of Triple-Network Crosslinking

Hanwei Zhang,<sup>1</sup> Amy Betz,<sup>2</sup> Aisha Qadeer,<sup>3</sup> Daniel Attinger,<sup>2</sup> Weiliam Chen<sup>1</sup>

<sup>1</sup>Division of Wound Healing and Regenerative Medicine, Department of Surgery, New York University School of Medicine, New York, New York 10016

<sup>2</sup>Mechanical Engineering Department, Columbia University, New York, New York 10027

<sup>3</sup>Endomedix, Inc., NJIT Enterprise Development Center, Newark, New Jersey 07103

Received 26 October 2010; accepted 12 December 2010

DOI 10.1002/app.34001

Published online 31 March 2011 in Wiley Online Library (wileyonlinelibrary.com).

**ABSTRACT:** A microfluidic emulsification method for producing monodispersed microgels from a triple interpenetrating network (3XN) hydrogel was reported. This 3XN system is comprised of minimally modified natural GRAS materials, partially oxidized dextran (Odex), Teleostean, and *N*-carboxyethyl chitosan (CEC), without the need of utilizing extraneous crosslinkers or photo-initiators, which has been proved to be a novel biodegradable and mechanically strong *in-situ* gelable hydrogel systems. A microfluidic chip was specifically designed to produce microgels from the 3XN hydrogel system. The study

shows that microfluidic emulsification method could yield microgels with better size and morphology than the conventional in-emulsion-crosslinking method, and the size of microgels could be modulated by simply adjusting the flow rates of the oil and/or the individual precursor fluids. © 2011 Wiley Periodicals, Inc. *J Appl Polym Sci* 121: 3093–3100, 2011

**Key words:** microfluidic emulsification method; monodispersed microgels; triple interpenetrating network (3XN) hydrogel; oxidized dextran; teleostean; chitosan

## INTRODUCTION

Hydrogels are hydrophilic three-dimensional polymer networks, crosslinked chemically and/or physically, capable of retaining a large amount of water.<sup>1,2</sup> The potentials of utilizing spherical hydrogel micro-particles (MPs), or microgels as delivery vehicles for small molecules, macromolecules, and cells have been explored.<sup>3–5</sup> By tailoring the properties of MPs, both the release-rate and release-profile of drug molecules can be optimized to for specific applications. The most important properties of MPs are their size and morphology. It has been shown that using monodispersed MPs in drug delivery systems or sensing applications are advantageous over their polydispersed counterparts with respect to monitoring, predicting, and modeling of their behavior as they exhibit a constant and more predictable response to external stimuli.<sup>6–8</sup> Currently, there is no general method available for the formulation of monodispersed hydrogel MPs. Conventional methods to formulate MPs typically involve bulk emulsions formation by mechanically shearing of monomer solutions or precursors into a discontinuous, immiscible phase, followed by the polymerization of

the emulsified droplets. This process inevitably results in forming highly polydispersed particles.<sup>6,9</sup>

Methodologies aiming to formulate MPs of more controlled size have been reported, and these include: (i) supercritical fluid mediated technology,<sup>10</sup> (ii) precipitation,<sup>11</sup> (iii) micronozzle array,<sup>12</sup> (iv) electrostatically mediated techniques,<sup>13</sup> (v) micronozzle channel emulsification,<sup>14</sup> and (vi) membrane emulsification.<sup>15</sup> Microfluidic methods have been explored as alternatives to formulate MPs with more precisely controlled size distributions.<sup>8,16–18</sup> Typical microfluidic preparation of MPs follows the flow focusing technique; uniform streams of droplets have been produced with standard coefficients of variation on the diameter (CV) lower than 3%.<sup>4,19,20</sup> For instance, Nie et al.<sup>20</sup> used water as the continuous phase and oil as the dispersed phase at viscosity ratios of up to 500; high-viscosity droplets were formed by a flow focusing device and their sizes were in the same order of the nozzle size (i.e., 80 μm). Virtually all the MPs prepared by microfluidic methods are single precursor based (e.g., Ca-alginate), photo-polymerization or one-step reaction systems normally require potentially cytotoxic extraneous crosslinkers or photo-initiators.<sup>6,16–19</sup> Moreover, the MPs produced generally have poor mechanical properties<sup>8,17</sup> rendering them less appealing for certain biomedical applications. Developing hydrogel MPs with high mechanical strength, while avoiding using potentially cytotoxic modifiers, remains a challenge.

Correspondence to: W. Chen (weiliam.chen@nyumc.org).

Formation of interpenetrating polymer networks is an important strategy to enhance the overall mechanical strengths of hydrogels<sup>21,22</sup> because of the intrinsic difficulties in modulating the development of interpenetrating networks; it is difficult to prepare MPs using both conventional or microfluidic methods, this is likely the reason that MPs prepared from these complicated interpenetrating network hydrogel systems has not hitherto been reported. The goal of this investigation is to demonstrate the feasibility of using a microfluidic method to prepare monodispersed MPs from a novel biodegradable and mechanically strong *in-situ* gelable triple-interpenetrating networks (3XN) systems reported by us.<sup>23</sup> This 3XN system is comprised of minimally modified natural GRAS materials, partially oxidized dextran (Odex), Teleostean, and *N*-carboxyethyl chitosan (CEC), without the need of utilizing extraneous crosslinkers or photo-initiators. A microfluidic chip was specifically designed to produce spherical MPs from the 3XN hydrogel system. The viscosities of these three fluids (Teleostean, Odex, and CEC) are 0.347, 0.01, and 0.558 Pa s, respectively, and the target particle size is in the range of 10–100  $\mu\text{m}$ . The 3XN hydrogel MPs formulated have narrow size distribution, and their size can further be modulated by simply adjusting the flow rates of the individual precursor fluids.

## EXPERIMENTAL

### Materials

Dextran (from *Leuconostoc mesenteroides*,  $M_w = 76,000$ ), teleostean, chitosan (deacetylation degree 85%,  $M_w 750,000$ ), sodium periodate, sodium hydroxide, and acrylic acid were purchased from Sigma-Aldrich (St. Louis, MO). Dialysis tubing (MWCO 3500 and 6000) was from Thermo-Fisher (Hampton, NH). All other chemicals were of reagent grade. Deionized and distilled water was used.

### Material synthesis and rheological characterization of hydrogels

CEC (substitution degree  $\sim 45\%$ )<sup>24</sup> and Odex (oxidation degree 20%)<sup>1</sup> were prepared following previously described methods. Desired amounts of Odex, Teleostean, and CEC were dissolved in PBS (0.01M, pH = 7.4) to form their aqueous solutions, respectively; Odex/Teleostean/CEC hydrogels were prepared by first thoroughly mixing the Odex solution with the Teleostean solution, and allowed to react for approximately 30–60 s. CEC solution was subsequently blended with the Odex/Teleostean mixture (the volume ratio of Odex/Teleostean/CEC was

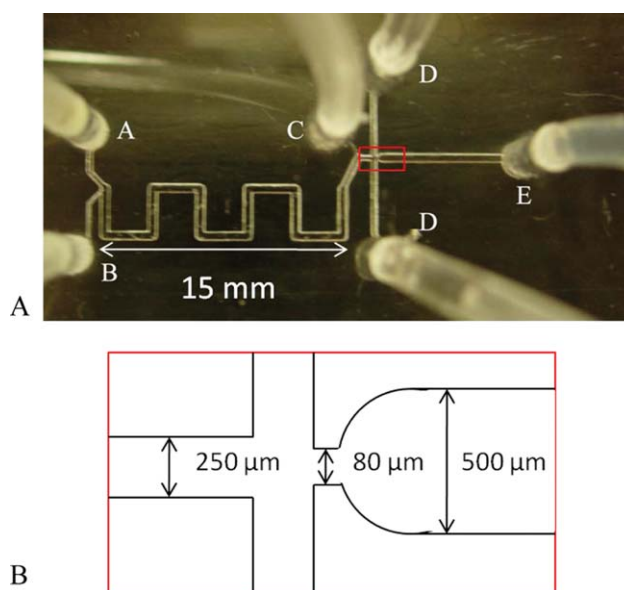


**Figure 1** Microfluidic chip (A) and close up of nozzle geometry (B). [Color figure can be viewed in the online issue, which is available at [wileyonlinelibrary.com](http://www.interscience.wiley.com)]

2 : 1 : 1) by gentle stirring for 10 s; the blend was maintained at 37°C.

All rheological characterizations of hydrogel formation were performed on a rheometer (HAAKE RS600, Thermo-Fisher, Hampton, NH). The storage moduli  $G'$ , loss moduli  $G''$ , and the complex viscosity  $\eta^*$  of the mixed system were monitored as a function of time at a frequency of 1 rad/s and a stress-strain of 2% under a constant temperature of 37°C.

### Fabrication of microfluidic chip

The chip was produced by milling channels in an acrylic plastic block. As depicted in Figure 1, the chip geometry was drawn in computer-aided-design software (Pro-E, Wildfire), which automatically generated the sequence of operations for the milling process. The channels were machined using a Minitech CNC milling machine, with a repeatability of 3  $\mu\text{m}$ . Millbits with diameter ranging from 80 to 500  $\mu\text{m}$  were used. All channels were 100  $\mu\text{m}$  deep. Inlet and outlet ports were drilled through the acrylic slab at 2.3 mm deep; these ports provide a leak-free interfacing for pushed-in Tygon tubing. Once finished, the chip was sonicated and inspected under a stereomicroscope to remove burrs and particulates. The channels were sealed with 80  $\mu\text{m}$  thick transparent tape (Adhesives Research); this configuration could withstand pressures up to 2 bars without leakage.

### The microfluidic emulsification method

The oil phase and precursor solutions were independently infused into the microchannels using a

digitally controlled syringe pump (PHD 2000, Harvard Apparatus, Holliston, MA). Odex, Teleostean, and CEC solutions (at a volume ratio of 2 : 1 : 1) were injected separately from inlets A, B, and D, respectively, [Fig. 1(A)], these streams would then converge to form a uniform stream; this steady flowing stream was then broken up by the shearing of the oil flow injected bidirectionally from inlet D to form polymer droplets [Fig. 1(A)]; these droplets exited from outlet E and were collected in the reservoir containing an oil phase (50 mL mineral oil with 0.5 mL of Span-80 added as an emulsifier), as shown in Figure 3, and allowed to auto-crosslink under constant stirring at 250 rpm (LR400 Lab Stirrer, Yamato, Tokyo, Japan). The reservoir was maintained at 37°C overnight to enable partial dehydration of the MPs formed. Subsequently, the MPs were recovered by precipitation; 60 mL of cold isopropanol was added to the mixture at room temperature while stirring, after 5 min, the mixture was centrifuged (5000 rpm) to separate the organic phase and it was discarded. The residual organic phase was extracted by washing the microspheres collected three times with approximately 20 mL of an acetone/isopropanol (1 : 1 ratio) cosolvent mixture. The 3XN MPs were recovered by air drying overnight at room temperature.

For comparison, 3XN MPs were also prepared by a conventional bulk in-emulsion-crosslinking method previously described by us.<sup>3</sup> In brief, aqueous Teleostean and CEC solutions (0.25 mL each) were mixed with 0.5 mL of an aqueous Odex solution. The mixture was then added to 50 mL of mineral oil (with 0.5 mL of Span 80 added as an emulsifier), maintained at 37°C, while under rapid agitation at 1000 rpm it was incubated overnight to form an emulsion. The MPs formed were recovered following a similar method described earlier.

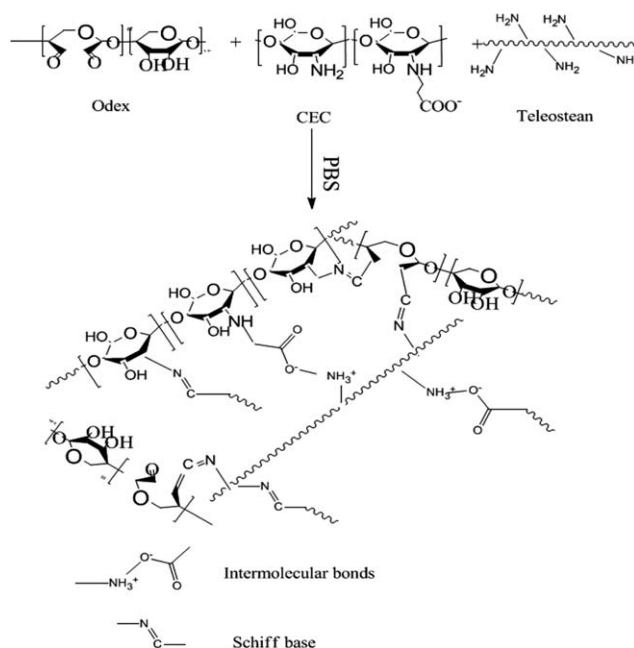
### Characterization of 3XN MPs

The dried MPs were secured on an aluminum stub with copper tapes and sputtered with gold; their morphologies were examined by a scanning electron microscope (SEM) (SFEG Leo 1550, AMO GmbH, Aachen, Germany) at 20 kV.<sup>3</sup> The mean size and size distribution of the fabricated MPs were characterized by a dynamic light scattering system (DLS), using a 90 Plus Particle Size Analyzer (Brookhaven Instruments Corp.) at 25°C with angle detection of 90° for 300 s.

## RESULTS AND DISCUSSION

### Design and synthesis of 3XN hydrogels

CEC is amphiphilic with both  $-\text{NH}_2$  and  $-\text{COOH}$ ; Odex through its  $-\text{CHO}$  functionalities serves as a



**Scheme 1** Schematic representation of the formation of the triple-network hydrogel.

macromolecular crosslinker for materials with free  $-\text{NH}_2$ ; thus, Odex can crosslink both Teleostean and CEC.<sup>1,25</sup> Besides, Odex, Teleostean, and CEC are all very abundant in  $-\text{OH}$ ,  $-\text{COOH}$ , and  $-\text{NH}_2$  groups capable of forming highly interactive secondary and tertiary structures.<sup>23,26,27</sup> Blending of solutions of Odex, Teleostean, and CEC formed a transparent hydrogel quickly, this rapid gelation property was attributable to the physical interactions of the secondary/tertiary structures, in concert with the chemical crosslinkings via Schiff base formation between the  $-\text{CHO}$  on Odex and the  $-\text{NH}_2$  on both CEC and Teleostean. The disparity in the reaction times and the modes of interaction between the three components resulted in the formation of multiple and interpenetrating networks (illustrated in Scheme 1). The theoretical aspects of the interaction between these components were collectively discussed by us in greater detail.<sup>1,23,28,29</sup>

The rheological properties of the 3XN hydrogel were determined at 37°C. Figure 2 depicted the temporal evolution of the elastic modulus ( $G'$ ) and viscous modulus ( $G''$ ) as well as the complex viscosity ( $\eta^*$ ) of hydrogel formation for a typical Odex/Teleostean/CEC composition (concentrations: 7.5%, 20%, and 2.5% (w/v), respectively) (volume ratio 2 : 1 : 1) at 37°C. Initially, when the  $G'$  was lower than the  $G''$ , the system exhibited the typical behavior of viscous fluids. When  $G'$  and  $G''$  crossed over, the system progressively transitioned to an elastic behavior dominated solid phase; this transition was defined as the gel point ( $t_{\text{gel}}$ ). Both moduli of the system continued to increase and eventually leveled off,

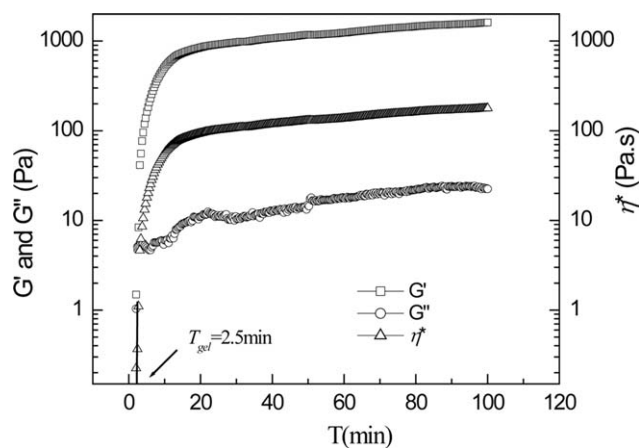


**Figure 2** Time evolution of the storage modulus ( $G'$ ) and the loss modulus ( $G''$ ) of a typical triple network hydrogel formulation composed of 7.5% Odex/20% teleostean/2.5% CEC (ratio 2 : 1 : 1). The crossover of  $G'$  and  $G''$  is denoted as the  $t_{gel}$  (gelation point).

signifying the formation of a well-developed three-dimensional network. The  $\eta^*$  also underwent a similar process; as shown in Figure 2, a rapid buildup at the beginning followed by level-off.

Blending Odex, teleostean, and CEC solutions of different concentrations resulted in the formation of hydrogels with different physicomechanical properties. Their rheological profiles (data not shown) were generally comparable to the one shown in Figure 2, but their  $t_{gel}$  and mechanical properties were vastly different and the results were summarized in Table I. In general,  $t_{gel}$  shortened rapidly with the increase of the precursor solution concentration with corresponding gradual increase in their mechanical strengths. Theoretically, a higher precursor solution concentration implies a greater abundance of reactive groups ( $-\text{CHO}$ ,  $-\text{NH}_2$ ,  $-\text{COOH}$ , etc.) in the mixture at closer proximity; leading to the acceleration of the rate of the crosslinking reaction (i.e., three-dimensional network formation) and the crosslink density of the system, thus greater mechanical strength. It should also be pointed out that the  $\eta^*$  of the precursor solutions elevated with their concentrations, especially with the CEC solution. For example, when the CEC concentration was increased

from 2.5 to 5%, the  $\eta^*$  increased from about 0.5 to 3.5 Pa s.

Most hydrogels, particularly those formulated entirely from natural materials, share the common characteristic of a lack of mechanical toughness, thereby, limiting the span of their potential biomedical applications.<sup>30</sup> High mechanical strength is one of the most important physical attributes of the 3XN hydrogel, and thus the MPs formulated. Although the mechanical strengths of the MPs produced could be improved by increasing the precursor concentrations, this type of maneuvers also requires precursor solutions of higher viscosities, in particular, the CEC solution, which inevitably accelerates the reaction. However, the results of our studies and other reports have demonstrated that higher viscosity would impede the mixing and flowing of the precursor solutions, increasing the pressure inside the microchannels, rendering it very difficult for the fluid to disperse to form droplets.<sup>31–33</sup> The rapid reaction also considerably increases the likelihood of blockade of the channels in the chip. Collectively, these factors greatly increased the level of difficulty for maneuvering. In our study, the most optimal concentration for Odex/Teleostean/CEC was established as 7.5%, 20%, and 2.5% (w/v), respectively.

#### Formation of microspheres of narrow size distribution by microfluidic emulsification

Our design of microfluidic emulsion formation was divided into two stages. The first stage was blending of the three precursors. To produce the desired MPs, the microfluidic device needs to generate drops containing three reagents; therefore, good mixing between the fluids of the dispersed phase is important. The flow in microchannels is usually laminar due to the low Reynolds number; hence, mixing is diffusion-limited. As shown in Figure 1, a y-connection and a 33-mm serpentine channel were used to mix the Teleostean (inlet A) and Odex (inlet B) solutions. The serpentine geometry was aimed at increasing the mixing time while keeping the overall dimension of the microfluidic chip within a reasonable range. The height and width of the serpentine

**TABLE I**  
The Main Rheological Properties of 3XN Hydrogels at 37°C

Formulation	Concentration (%w/v) Odex/CEC/teleostean	The solution of $\eta^*$ (Pa s) Odex/CEC/teleostean	$t_{gel}$ (min)	$G'$ (Pa)	$\eta^*$ (Pa s)
1	15/5/40	0.021/3.50/0.731	1.5	3500	410
2	7.5/2.5/20	0.01/0.558/0.347	2.5	1600	180
3	3.75/1.25/10	0.01/0.119/0.207	5	500	80

The  $G'$  and  $\eta^*$  were registered at 100 min.

The volume ratio of Odex/CEC/teleostean is 2:1:1.

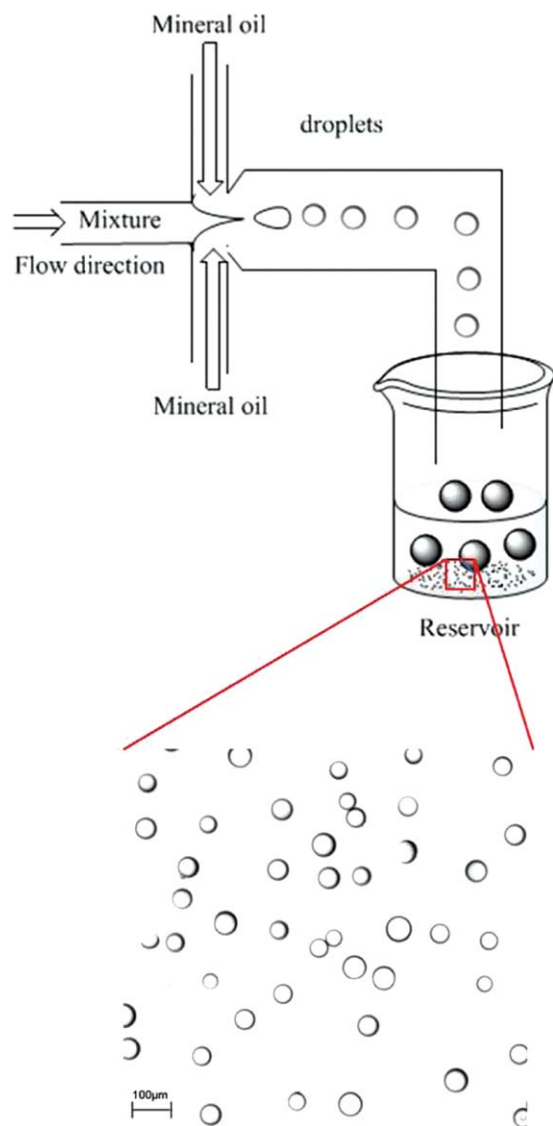


**Figure 3** Microfluidic formation of MPs and the corresponding microscopic image. [Color figure can be viewed in the online issue, which is available at [wileyonlinelibrary.com](http://wileyonlinelibrary.com).]

channel,  $h = 100 \mu\text{m}$  and  $w = 500 \mu\text{m}$ , were chosen so that the measured pressure drop was less than 2 bar at a filling velocity of 17 mm/s. To estimate the pressure drop, we assumed a straight channel with the total length of the serpentine channel, 33 mm. We used the correlation  $\Delta p = 12\mu LQ/[h^3w \cdot (1 - 0.63h/w)]$  for channels with rectangular cross section.<sup>34</sup> The viscosity of the mixture was conservatively assumed to be the measured viscosity of the most viscous of the two fluid, Teleostean,  $\mu = 0.347 \text{ Pa s}$ . At low Reynolds numbers, the turns in the serpentine channel are not expected to significantly increase the pressure drop.<sup>35</sup> The typical diffusion time needed to mix the reagents can be estimated as  $\tau = (w/2)^2/D$ . Assuming  $D = 1 \times 10^{-9} \text{ m}^2/\text{s}$ , which is the water diffusion coefficient of molecules of 2 Å

in size, we obtain  $\tau = 63 \text{ s}$ , corresponding to an operation velocity of 0.5 mm/s or a flow rate of 1.5  $\mu\text{L}/\text{min}$ . CEC solution was then injected from inlet C in Figure 1, mixing with the Odex/Teleostean blend to form the final blend. The second stage is the “necking/breaking” of this flowing mixture with the shear force created by the oil flow (inlet D), stretching the fluid stream at the junction causing necking, and finally breaking to form a steady stream of individual droplets (Fig. 3). Formation of droplets was the result of a balance between the viscous stresses produced by the perpendicularly intersected flow field, and the capillary stresses due to the surface tension between the two immiscible phases.<sup>16</sup> The droplets were collected in the reservoir under stirring at 37°C to facilitate crosslinking and subsequent water evaporation led to the formation of stable MPs not prone to aggregation. Figure 3 also depicted the image of the prepared MPs in the oil phase under optical microscopy, their near uniform sizes and bead-shaped morphology was self-evident.

#### Modulation of the physical attributes of microspheres

The 3XN MPs were prepared by microfluidic method at the precursor (represented by CEC) and the oil flow rates of 50 and 500  $\mu\text{L}/\text{min}$ . For comparison, 3XN MPs were also prepared by a conventional bulk in-emulsion-crosslinking method. Figure 4 showed the scanning electron microscopy (SEM) images of typical MPs formulations prepared by, (A) the microfluidic method, and (B) the conventional in-emulsion-crosslinking method; the MPs prepared by the former were considerably more uniform in both sizes and shapes compared to those prepared by the latter. Moreover, many of the microspheres formed were irregular beads with random morphology. The size distribution profiles and mean radii for typical 3XN MPs were determined by dynamic light scattering, and the results were shown in Figure 5. Both DLS showed single symmetric profiles, but their size distributions were evidently different. MPs produced by the microfluidic method had a narrow size distribution with an average radius of  $28.5 \pm 2.0 \mu\text{m}$  (standard deviation as a percentage: 7.0%), further confirming their near monodispersity. In contrast, the MPs produced from the conventional in-emulsion-crosslinking method had a considerably wider size distribution with an average radius of  $10 \pm 3.7 \mu\text{m}$  (standard deviation as a percentage: 35%).

As the concentrations of the three precursor solutions were fixed, both the precursor and oil flow rates were the primary factors in determining the size distribution of the MPs formed. Figure 6 showed typical SEM images and DSL plots of various MP formulations when the oil flow changed

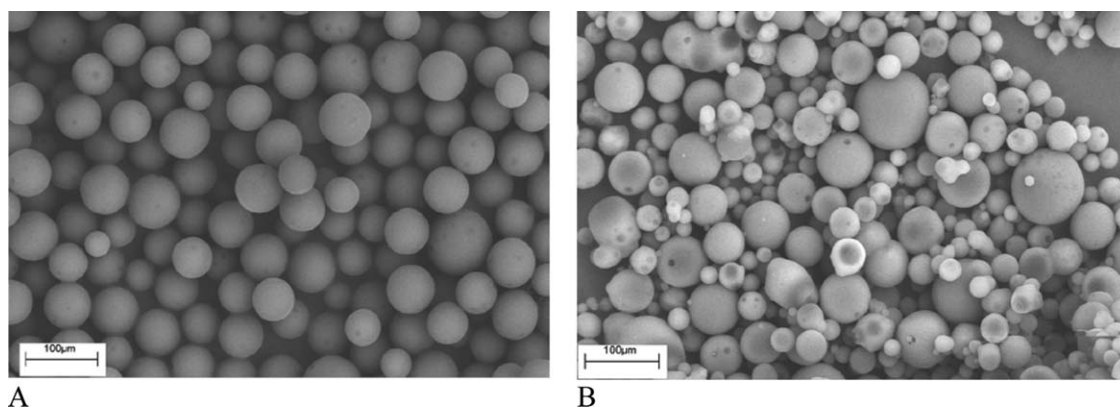


**Figure 4** The SEM images of 3XN MPs prepared by (A) microfluidic method and (B) conventional bulk in-emulsion-crosslinking method.

from 250, 500, and 750  $\mu\text{L}/\text{min}$ , while the precursor (represented by the CEC) solution flow rate was maintained at 50  $\mu\text{L}/\text{min}$ . The SEM images (A, B, and C) showed that all formulations had relatively uniform sizes and spherical morphology. Importantly, adjustment of the oil flow rate effectively changed the size of the 3XN MPs formed, and their size decreased gradually with the increase of flow. In addition, all the samples showed single and narrow symmetric DSL profiles, further implicating the narrow size distributions of all the MPs produced. Their mean radii were  $18.2 \pm 2.7$ ,  $28.5 \pm 2.0$  to  $50.5 \pm 4.5$   $\mu\text{m}$ , at the oil flow rates of 750, 500 to 250  $\mu\text{L}/\text{min}$ , respectively.

Briefly, the flow-focusing mechanism generated drops of that precursor fluid in a continuous phase of mineral oil with its viscosity  $\mu = 0.0276$  Pa s and a volumic mass  $\rho = 840$   $\text{kg}/\text{m}^3$ , using Span 80 as the surfactant. The main parameter used to control the drop size was the flow rate of the mineral oil: it was varied from 250 to 750  $\mu\text{L}/\text{min}$  to produce MPs with radii in the range of 18–50  $\mu\text{m}$ . The MPs prepared from the microfluidic device had typical CV  $< 9\%$ . This is about four times better than the CV of 35% obtained in this study by the in-emulsion-crosslinking method, indicating the obvious improvement on the size control of the prepared MPs. As demonstrated here, preparation of MPs was affected by the reaction of the precursors (i.e., gelation time, mechanical properties, etc.) and the formation of droplets (agitation speed, reactor geometry, etc.). Utilizing the conventional in-emulsion-crosslinking method, partitioning of the precursor solution into droplets by shear force accompanying the crosslinking reaction of the precursors resulted in the constant changing of the formation condition of the droplets. The gradual change in the mechanical properties of the precursor mixture in concert with the crosslinking reaction resulted in the unstable formation condition of the droplets, which eventually

contributed to the wide particle size distribution of the MPs formed and their nonuniform morphology.<sup>3,36</sup> In contrast, formation of droplets by the microfluidic method was through a flow-focusing mechanism, which was the result of a calibrated balance between viscous stresses and capillary stresses, attained constant as soon as the rates of precursor flow and oil flow stabilized.<sup>16</sup> Thus, the microfluidic method allowed more precise control of the MP formation leading to the more uniformly-dispersed MPs. Undoubtedly, achieving CV  $< 9\%$  using the microfluidic method was a considerable improvement compared to its counterpart prepared by the conventional technique, however, a CV below 5% had been reported.<sup>23,36,37</sup> It should be noted that a major distinction between these studies and the investigation described here is the magnitude of the

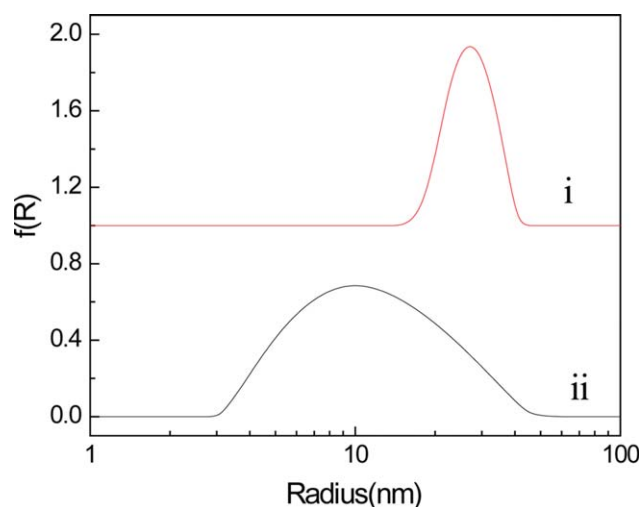


**Figure 5** The size distributions of the MPs produced by (i) microfluidic method (coefficient of variation: 7%), and (ii) conventional bulk in-emulsion-crosslinking methods (coefficient of variation: 35%). [Color figure can be viewed in the online issue, which is available at [www.interscience.wiley.com](http://www.interscience.wiley.com).]

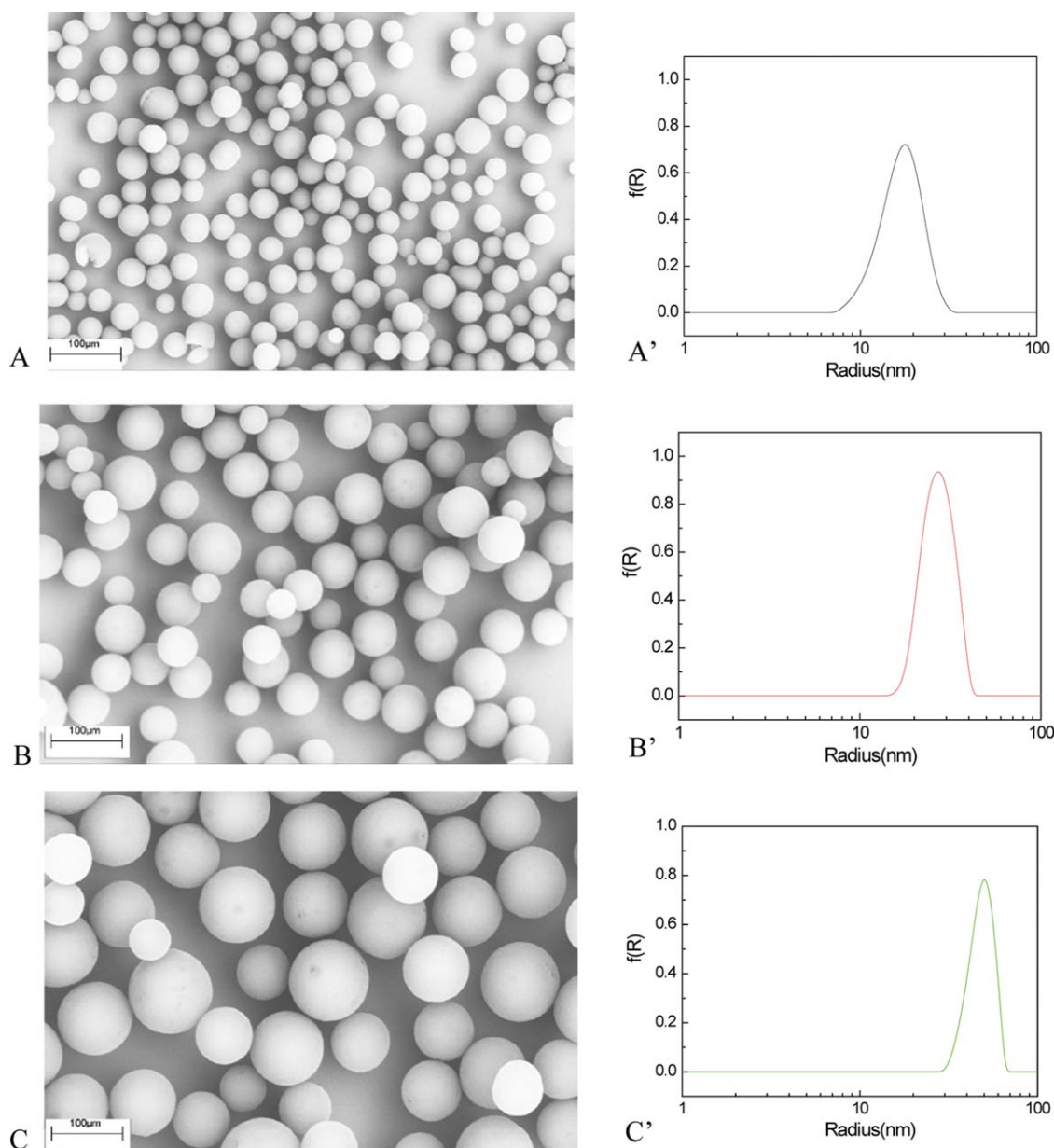


**Figure 6** SEM images and size distributions of the MPs produced under different oil flow rates: (A) 750  $\mu\text{L}/\text{min}$ , (B) 500  $\mu\text{L}/\text{min}$ , and (C) 250  $\mu\text{L}/\text{min}$ . [Color figure can be viewed in the online issue, which is available at [wileyonlinelibrary.com](http://wileyonlinelibrary.com).]

capillary number. The capillary number ( $Ca$ ) relates the viscous forces and surface tension across two immiscible interfaces, it is defined as  $Ca = \mu v / \sigma$ , where  $\mu$  is the viscosity of the liquid,  $\sigma$  is the interfacial tension, and  $v$  is defined as the volumetric flow rate divided by the cross-sectional area of the nozzle.<sup>23</sup> When the  $Ca$  of the continuous and dispersed phase is negligible (i.e.,  $Ca \leq 0.1$ ), the drops are generated in squeezing and dripping modes, two breakup processes that are generally very stable. In our study, however, assuming a  $\sigma$  of 20 mN/m and a  $\mu$  of 0.3 Pa s for the dispersed phase, the capillary number for the continuous and dispersed phase is approximately one, a value where less stable genera-

tion has already been reported.<sup>38</sup> Another possible cause for the higher CV obtained in our microfluidic experiments could also be the associated chemical reaction with changing physicochemical characteristics; this issue certainly warrants further investigation. The effect of precursor solutions' flow rates on the MPs produced was also evaluated; the oil flow rate was maintained at 500  $\mu\text{L}/\text{min}$  while the precursor (represented by CEC) solution flow rate changed incrementally from 25, 50 to 100  $\mu\text{L}/\text{min}$ , the MPs produced were comparable with relatively uniform size distributions (SEM images not shown). The DSL profiles of these MPs were depicted in Figure 7; their mean radii increased from  $18.1 \pm 1.5$ ,

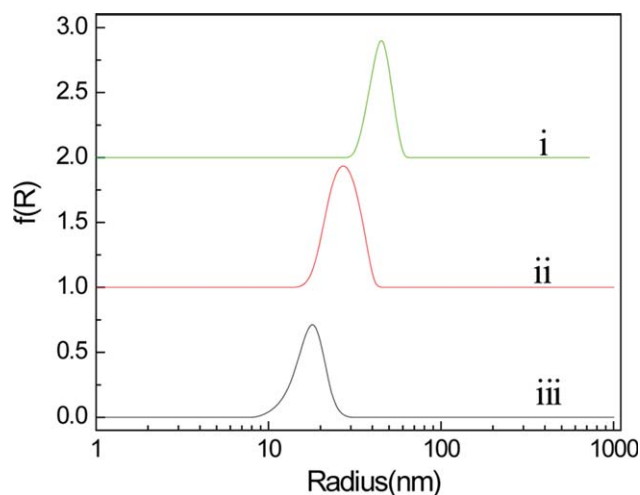


**Figure 7** Size distributions of the MPs produced by different CEC flow rates: (i) 100  $\mu\text{L}/\text{min}$ , (ii) 50  $\mu\text{L}/\text{min}$ , and (iii) 25  $\mu\text{L}/\text{min}$ . [Color figure can be viewed in the online issue, which is available at [wileyonlinelibrary.com](http://wileyonlinelibrary.com).]

28.5  $\pm$  2.0 to 45.6  $\pm$  5.0  $\mu\text{m}$ , when the precursor solution flow rate was elevated from 25, 50 to 100  $\mu\text{L}/\text{min}$ , respectively.

## CONCLUSIONS

In summary, we have reported a method for producing monodispersed microgels from a triple interpenetrating network hydrogel via microfluidic emulsification. These microgels are composed of naturally derived materials without the need of utilizing any extraneous small molecule crosslinkers. By controlling the flow rates of the oil and/or the precursors, we have achieved control over the size of the microgels and their morphology. Importantly, microfluidic emulsification yields particles with better size and morphology than the conventional in-emulsion-crosslinking method. We have previously demonstrated the high mechanical strength of the triple network hydrogel composed of the same ingredients (i.e., chitosan, dextran and Teleostean), it could thus be inferred that the microgels prepared also assume a comparable level of mechanical strength.

## References

- Weng, L.; Chen, X.; Chen, W. *Biomacromolecules* 2007, 8, 1109.
- Singh, A.; Suri, S.; Roy, K. *Biomaterials* 2009, 30, 5187.
- Weng, L.; Ivanova, N. D.; Zakhaleva, J.; Chen, W. *Biomaterials* 2008, 29, 4149.
- Franzese, G. T.; Ni, B.; Ling, Y. B.; Khademhosseini, A. *J Am Chem Soc* 2006, 128, 15064.
- Cohen, J. A.; Beaudette, T. T.; Tseng, W. W.; Bachelder, E. M.; Mende, I.; Engleman, E. G.; Fréchet, J. M. *Bioconjug Chem* 2009, 20, 111.
- De Geest, B. G.; Urbanski, J. P.; Thorsen, T.; Demeester, J.; De Smedt, S. C. *Langmuir* 2005, 21, 10275.
- Cai, T.; Marquez, M.; Hu, Z. *Langmuir* 2007, 23, 8663.
- Zhang, H.; Tumarkin, E.; Peerani, R.; Nie, Z.; Sullan, R. M.; Walker, G. C.; Kumacheva, E. *J Am Chem Soc* 2006, 128, 12205.
- Charcosset, C.; Fessi, H. *Rev Chem Eng* 2005, 21, 1.
- Sarkari, M.; Darrat, I.; Knutson, B. L. *Biotechnol Prog* 2003, 19, 448.
- Zhu, H. G.; Stein, E. W.; Lu, Z. H.; Lvov, Y. M.; McShane, M. *J Chem Mater* 2005, 17, 2323.
- Sugiura, S.; Oda, T.; Izumida, Y.; Aoyagi, Y.; Satake, M.; Ochiai, A.; Ohkohchi, N.; Nakajima, M. *Biomaterials* 2005, 26, 3327.
- Berkland, C.; Kim, K.; Pack, D. W. *J Control Release* 2001, 73, 59.
- Iwamoto, S.; Nakagawa, K.; Sugiura, S.; Nakajima, M. *AAPS Pharm Sci Tech* 2002, 3, article 25.
- Liu, X. D.; Bao, D. C.; Xue, W. M.; Xiong, Y.; Yu, W. T.; Yu, X. J.; Ma, X. J.; Yuan, Q. *J Appl Polym Sci* 2003, 87, 848.
- Yu, Z. Y.; Chen, L.; Chen, S. *J Mater Chem* 2010, 20, 6182.
- Rondeau, E.; Cooper-White, J. J. *Langmuir* 2008, 24, 6937.
- Steinbacher, J. L.; Moy, R. W.; Price, K. E.; Cummings, M. A.; Roychowdhury, C.; Buffy, J. J.; Olbricht, W. L.; Haaf, M.; McQuade, D. T. *J Am Chem Soc* 2006, 128, 9442.
- Seo, M.; Nie, Z.; Xu, S.; Mok, M.; Lewis, P. C.; Graham, R.; Kumacheva, E. *Langmuir* 2005, 21, 11614.
- Nie, Z. H.; Seo, M. S.; Xu, S. Q.; Lewis, P. C.; Mok, M.; Kumacheva, E.; Whitesides, G. M.; Garstecki, P.; Stone, H. A. *Microfluid Nanofluid* 2008, 5, 585.
- Yasuda, K.; Gong, J. P.; Katsuyama, Y.; Nakayama, A.; Tanabe, Y.; Kondo, E.; Ueno, M.; Osada, Y. *Biomaterials* 2005, 26, 4468.
- Weng, L.; Gouldstone, A.; Wu, Y.; Chen, W. *Biomaterials* 2008, 29, 2153.
- Zhang, H. W.; Qadeer, A.; Mynarcik, D.; Chen, W. *Biomaterials*, to appear.
- Jiang, H.; Wang, Y.; Huang, Q.; Li, Y.; Xu, C.; Zhu, K.; Chen, W. *Macromol Biosci* 2005, 5, 1226.
- Weng, L.; Romanov, A.; Rooney, J.; Chen, W. *Biomaterials* 2008, 29, 3905.
- Van Tomme, S. R.; Van Steenberg, M. J.; De Smedt, S. C.; Van Nostrum, C. F.; Hennink, W. E. *Biomaterials* 2005, 26, 2129.
- Van Tomme, S. R.; Hennink, W. E. *Expert Rev Med Devices* 2007, 4, 147.
- Peng, H. T.; Shek, P. N. *J Mater Sci Mater Med* 2009, 20, 1753.
- Van Tomme, S. R.; Van Nostruma, C. F.; de Smedt, S. C.; Hennink, W. E. *Biomaterials* 2006, 27, 4141.
- Nakayama, A.; Kakugo, A.; Gong, J. P.; Osada, Y.; Takai, M.; Erata, T.; Kawano, S. *Adv Funct Mater* 2004, 14, 1124.
- Choi, C. H.; Jung, J. H.; Rhee, Y. W.; Kim, D. P.; Shim, S. E.; Lee, C. S. *Biomed Microdevices* 2007, 9, 855.
- Yang, C. H.; Lin, Y. S.; Huang, K. S.; Huang, Y. C.; Wang, E. C.; Jhong, J. Y.; Kuo, Y. C. *Lab Chip* 2009, 9, 145.
- Tan, Y. C.; Lee, A. P. *Lab Chip* 2005, 5, 1178.
- Bruus, H. *Theoretical Microfluidics*; Oxford University Press: New York, 2008.
- Rosaguti, N. *Int J Heat Mass Transfer* 2006, 49, 2912.
- Lee, J. E.; Kim, K. E.; Kwon, I. C.; Ahn, H. J.; Lee, S. H.; Cho, H.; Kim, H. J.; Seong, S. C.; Lee, M. C. *Biomaterials* 2004, 25, 4163.
- Tan, S. H.; Sohel Murshed, S. M.; Nguyen, N.T.; Wong, T. N.; Yobas, L. *J Phys D: Appl Phys* 2008, 41, 165501.
- Utada, A.; Fernandez-Nieves, A.; Stone, H. A.; Weitz, D. A. *Phys Rev Lett* 2007, 99, 094502.